Ocean Roles in the TBO Transitions of the Indian–Australian Monsoon System

JIN-YI YU AND SHU-PING WENG

Department of Earth System Science, University of California, Irvine, Irvine, California

JOHN D. FARRARA

Department of Atmospheric Sciences, University of California, Los Angeles, Los Angeles, California

13 November 2002 and 28 February 2003

ABSTRACT

This study uses a series of coupled atmosphere–ocean general circulation model (CGCM) experiments to examine the roles of the Indian and Pacific Oceans in the transition phases of the tropospheric biennial oscillation (TBO) in the Indian–Australian monsoon system. In each of the three CGCM experiments, air–sea interactions are restricted to a certain portion of the Indo-Pacific Ocean by including only that portion of the ocean in the ocean model component of the CGCM. The results show that the in-phase TBO transition from a strong (weak) Indian summer monsoon to a strong (weak) Australian summer monsoon occurs more often in the CGCM experiments that include an interactive Pacific Ocean. The out-of-phase TBO transition from a strong (weak) Australian summer monsoon to a weak (strong) Indian summer monsoon occurs more often in the CGCM experiments that include an interactive Indian Ocean. The associated sea surface temperature (SST) anomalies are characterized by an ENSO-type pattern in the Pacific Ocean and basinwide warming/cooling in the Indian Ocean. The Pacific SST anomalies maintain large amplitude during the in-phase transition in the northern autumn and reverse their sign during the out-of-phase transition in the northern spring. On the other hand, the Indian Ocean SST anomalies maintain large amplitude during the out-of-phase monsoon transition and reverse their sign during the in-phase transition. These seasonally dependent evolutions of Indian and Pacific Ocean SST anomalies allow these two oceans to play different roles in the transition phases of the TBO in the Indian–Australian monsoon system.

1. Introduction

Long-term precipitation records show that the interannual variations of Indian summer monsoon rainfall have a tendency to display a quasi-biennial oscillation: years with above-normal summer rainfall tend to be followed by ones with below-normal rainfall and vice versa (Mooley and Parthasarathy 1984; Yasunari 1990; Clarke et al. 1998; Webster et al. 1998; Meehl and Arblaster 2002a). This tendency is often referred to the tropospheric biennial oscillation (TBO). The TBO tendency is also found in Australian summer monsoon rainfall (Ropelewski and Halpert 1987; Yasunari and Suppiah 1988; Meehl and Arblaster 2002a). The biennial tendencies in these two monsoon regions appear to be related. Meehl (1987, 1993) showed that interannual anomalies in convection (proxied by outgoing longwave radiation) starting nearby the Indian subcontinent in northern summer propagate southeastward and arrive in the Indonesia–northern Australia region during the succeeding autumn and winter. That is, a strong (weak) Indian summer monsoon is often followed by a strong (weak) Australian summer monsoon. The anomalies then reverse sign as they return to the Northern Hemisphere and lead to a weak (strong) Indian monsoon during the northern summer of the following year. The in-phase TBO transition from Indian to Australian monsoons during the northern autumn and the out-of-phase TBO transition from the Australian to Indian monsoons during the northern spring are two key features of the TBO in the Indian–Australian monsoon system.

Interactions between the atmosphere and the tropical Indian and Pacific Oceans have been postulated to play a central role in the TBO (e.g., Nicholls 1978; Meehl 1987, 1993; Clarke et al. 1998; Chang and Li 2000). Kim and Lau (2001) performed model experiments with and without an interactive Indian Ocean to demonstrate the contribution of the combination of ocean basin phenomena in the TBO. Meehl and Arblaster (2002b) used (Atmospheric Model Intercomparison Project) AMIP-type experiments to quantify contributions of anomalous sea surface temperatures (SSTs) in the respective Indian

Corresponding author address: Dr. Jin-Yi Yu, Department of Earth System Science, University of California, Irvine, Irvine, CA 92697-3100.
E-mail: jyyu@uci.edu

and Pacific Ocean basins to the TBO transitions. Tomita and Yasunari (1996) analyze TBO transitions in terms of western Pacific–Indian Ocean interactions. In particular, the recent observational study of Meehl and Arblaster (2002a) showed that the transition phases of the biennial tendency are accompanied by anomalous SSTs in the Indian and Pacific Oceans. Surface wind anomalies associated with the Indian summer monsoon initiate a reversal in the SST anomalies in the Indian Ocean, and the wind anomalies associated with the Australian summer monsoon reverse the sign of SST anomalies in the tropical Pacific Ocean. Their results suggest that the Indian–Australian monsoon system affects the Pacific and Indian Ocean SSTs differently. Therefore, feedbacks from these two oceans to the monsoon systems may play different roles in the transition phases of the biennial monsoon tendency. The current study aims to identify these different roles by performing experiments with a coupled atmosphere–ocean general circulation model (CGCM) that restricts atmosphere–ocean couplings to only the Indian or Pacific Oceans or both. Section 2 describes the CGCM and the experiments. The simulated Indian and Australian monsoons and their transitions are described in section 3. Section 4 links the TBO transitions to SST anomalies in the Indian and Pacific Oceans. The conclusions and discussion are given in section 5.

2. Model and experiments

The CGCM used in this study consists of the University of California, Los Angeles (UCLA) atmospheric GCM (AGCM) (Mechoso et al. 2000) and the Geophysical Fluid Dynamics Laboratory (GFDL) Modular Ocean Model (MOM; Bryan 1969; Cox 1984; see Yu and Mechoso 2001 for a detailed description of the CGCM). The AGCM is global with a horizontal resolution of 4° latitude by 5° longitude and 15 levels in the vertical. The oceanic model has a longitudinal resolution of 1°, a latitudinal resolution that varies gradually from 1/3° between 10°S and 10°N to about 3° at both 30°S and 50°N, and 27 layers in the vertical. Three CGCM experiments are performed in this study: the Indo-Pacific run, the Pacific run, and the Indian Ocean run. In the Pacific run, the CGCM includes only the tropical Pacific Ocean (30°S–50°N, 130°E–70°W) in the domain of its ocean model component. The Indian Ocean run includes only the Indian Ocean (30°S–50°N, 30°–130°E) in the ocean model domain. The Indo-Pacific run includes both the Indian and Pacific Oceans (30°S–50°N, 30°E–70°W) in the ocean model domain. Outside the oceanic model domains, SSTs and sea ice distributions for the AGCM are prescribed based on a monthly varying climatology. Inside the ocean model domains, SSTs poleward of 20°S and 30°N are relaxed toward their climatological values.

The Indo-Pacific, Pacific, and Indian Ocean runs are integrated for 59, 52, and 58 yr, respectively. Only the last 30 yr of the simulations are analyzed in this study. All three CGCM runs produce a reasonable SST climatology in the Pacific and Indian Oceans (not shown), with a warm pool (SST greater than 28°C) that covers both the tropical western Pacific and eastern Indian Oceans. Both the Indo-Pacific and Pacific runs produce large interannual SST variability (about 2°C for the largest events) in the tropical eastern Pacific, which resemble ENSO events in the observations (Yu et al. 2000; Yu and Mechoso 2001; Yu et al. 2002). The Indian Ocean and the Indo-Pacific runs also exhibit significant interannual SST variability (about 0.5°C) in the Indian Ocean (not shown).

3. Transitions between Indian and Australian summer monsoons

The simulated Indian and Australian monsoons from the Indo-Pacific run are compared with the observations in Fig. 1, which shows the mean rainfall and 850-mb winds during the northern summer monsoon season [June–September (JJAS)] and during the southern summer monsoon season [December–February (DJF)]. The Climate Prediction Center (CPC) Merged Analysis of Precipitation (CMAP; Xie and Arkin 1997) and the National Centers for Environmental Prediction–National Center for Atmospheric Research (NCEP–NCAR) reanalysis data (Kalnay et al. 1996) from 1979 to 2000 are used to construct the observed monsoon climatology. The observed Indian summer monsoon (Fig. 1a) is characterized by a rainfall maximum that extends from western India to the Bay of Bengal and a strong monsoon gyre that brings water vapor from the southern Indian Ocean into the India Peninsula along the east coast of Africa. The Indo-Pacific run reasonably reproduces both the rainfall and circulation patterns of the Indian summer monsoon (Fig. 1b). Due to the coarse horizontal resolution in the AGCM component, the simulated rainfall centers in western India and the Bay of Bengal are not as well separated as in the observations. The observed Australian summer monsoon (Fig. 1c) is characterized by heavy rainfall extending from the Maritime Continent toward northern Australia and a cyclonic circulation dipole pattern straddling the equator that transports water vapor from the subtropics into this region. These rainfall and circulation patterns are reasonably simulated in the Indo-Pacific run, except that the simulated rainfall maximum does not extend as far south as in the observations (Fig. 1d). Similar Indian and Australian summer monsoon simulations are produced by the Pacific and Indian Ocean runs (not shown).

We define two rainfall indices to represent the strength of the Indian and Australian monsoons. The Indian and Australian monsoon rainfall indices (IMRI and AMRI, respectively) are defined as the mean rainfall amounts averaged over the Indian (10°–30°N, 65°E–100°E) and Australian (20°S–5°N, 100°–150°E) monsoon regions, respectively. Their interannual anomalies

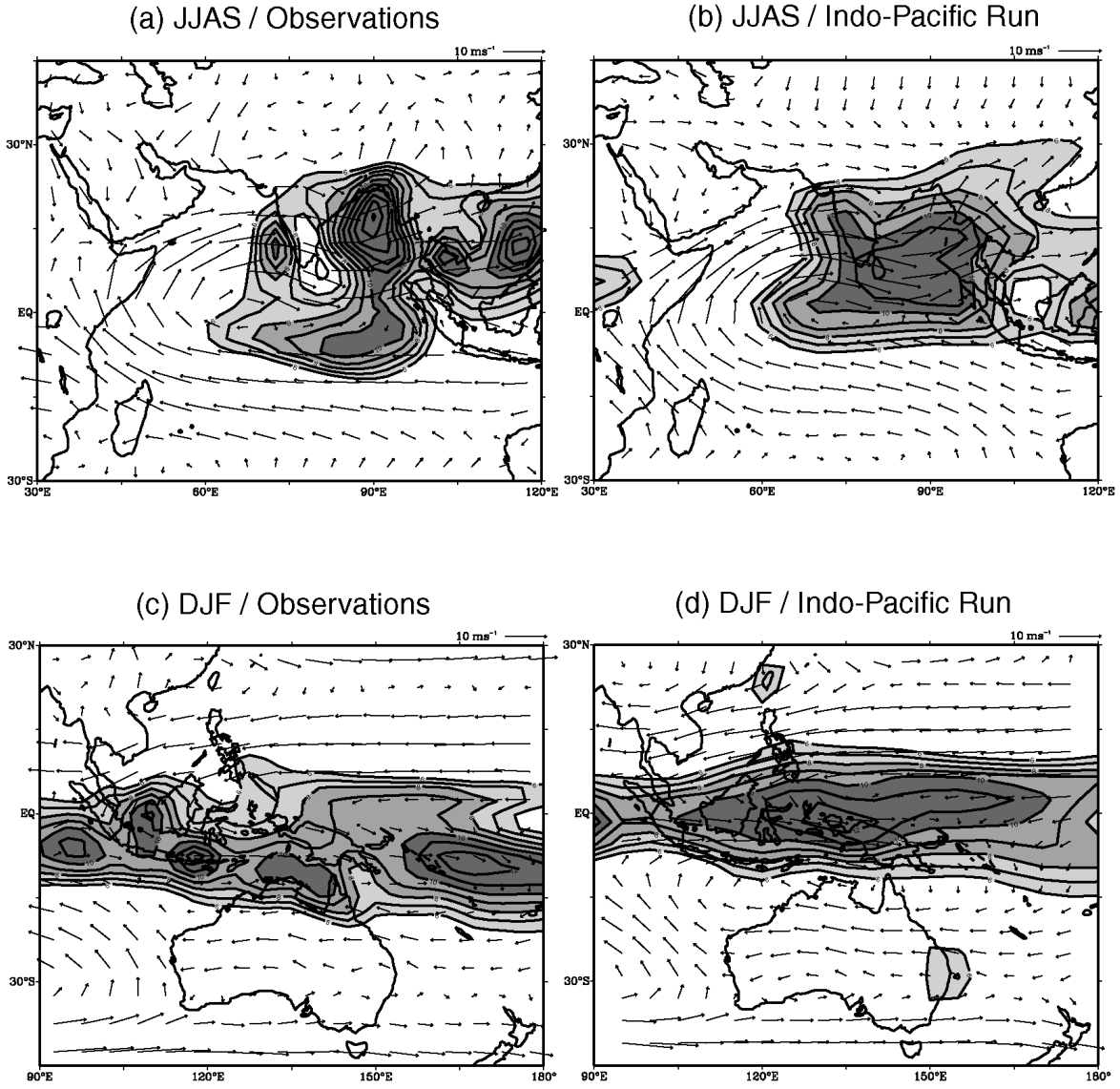

FIG. 1. Long-term mean precipitation and 850-mb winds for the (a), (b) India summer monsoon (JJAS) and Australian summer monsoon season (c), (d) DJF. Panels (a) and (c) are from observations; (b) and (d) are simulated by the Indo-Pacific run. Contour intervals are 1 mm day^{-1} for precipitation. Values greater than 6 mm day^{-1} are shaded.

are constructed by removing their respective long-term seasonal cycles. Figure 2 shows the interannual variations of the JJAS IMRI and the DJF AMRI calculated from the CMAP data and the three CGCM experiments. The values shown are normalized by their respective standard deviations. Based on these two indices, we identify the in-phase transition of the TBO as a strong (weak) Indian summer monsoon followed by a strong (weak) Australian summer monsoon, and the out-of-phase transition of the TBO as a strong (weak) Australian summer monsoon followed by a weak (strong) Indian summer monsoon in the next year. For the sake of discussion, we refer to the in-phase monsoon transition as the I-to-A transition and the out-of-phase monsoon transition as the A-to-I transition. If the amplitude of a normalized IMRI anomaly in one JJAS is 1) larger than 0.7 and 2) followed by a large (amplitude greater than 0.7) normalized AMRI value with the same sign in the DJF of the same year, this case is identified as an I-to-A transition case. Similarly, an A-to-I transition case is identified when a large (amplitude > 0.7) normalized AMRI anomaly in DJF is followed by a large (amplitude > 0.7) normalized IMRI anomaly with an opposite sign in JJAS of the next year. The threshold amplitude of 0.7 is used to select only transitions between large anomalous Indian and Australian monsoon seasons. We also tested two smaller threshold values (0.6 and 0.5) for the case identification and obtained similar results as those presented here for the threshold value of 0.7 (not shown).

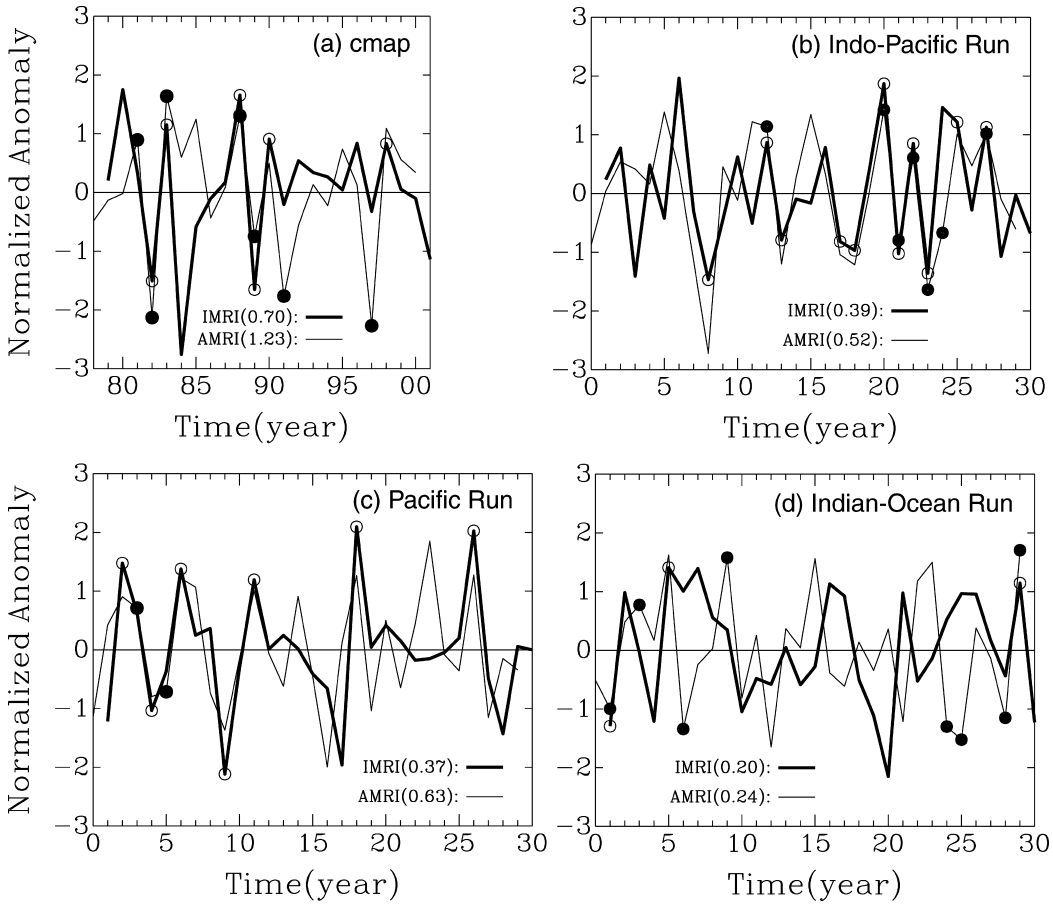

FIG. 2. Normalized interannual anomalies of monsoon rainfall indices for the Indian summer (JJAS) monsoon (IMRI; thick solid lines) and the Australian summer (DJF) monsoon (AMRI; thin solid lines): (a) the CMAP observation, (b) the Indo-Pacific run, (c) the Pacific run, and (d) the Indian Ocean run. The interannual anomalies are obtained by removing long-term mean seasonal cycle. The interannual anomalies are then normalized by their std devs. Std devs of IMRI and AMRI are indicated inside the parentheses of each panel. The time axis is ticked in the way that corresponds to the JJAS and its succeeding DJF season for the IMRI and AMRI, respectively. The opened and closed circles mark, respectively, the identified I-to-A and A-to-I transition cases. See text for the explanation for the selection of these cases.

The identified I-to-A and A-to-I transition cases are marked, respectively, by opened and closed circles in Fig. 2. For the sake of presentation, all identified I-to-A transitions are marked on the time series of the IMRI (the thick lines in Fig. 2) and all identified A-to-I transitions are marked on the time series of the AMRI (the thin lines). For example in the observations (Fig. 2a), the first I-to-A transition case occurs in 1982, which is marked by a opened circle in that year of the IMRI time series. In this year, the normalized JJAS IMRI value is below normal with a large amplitude of -1.5. This large below-normal Indian summer monsoon season is followed by a large below-normal Australian summer monsoon in DJF of the same year, whose normalized DJF AMRI anomaly is -2.1. The first A-to-I transition in the observations occurs in 1981, which is marked by a closed circle in that year of the AMRI time series. In this year, the large above-normal Australian monsoon (the normalized DJF AMRI anomaly is 0.9) is followed by a large below-normal Indian monsoon (the normalized JJAS IMRI anomaly is -1.5) in JJAS of 1982.

It is interesting to note that while both the observations (Fig. 2a) and the Indo-Pacific run (Fig. 2b) have comparable numbers of opened and closed circles, the Pacific run is dominated by opened circles (Fig. 2c) and the Indian Ocean run is dominated by closed circles (Fig. 2d). Table 1 summarizes the numbers of I-to-A and A-to-I transition cases identified in Fig. 2. The table indicates that the Pacific run produces mostly I-to-A transitions. Very few A-to-I transitions are produced in this run. On the other hand, the Indian Ocean run produces mostly A-to-I transition cases. The different preference suggests that an interactive Indian Ocean is crucial to the A-to-I transition while an interactive Pacific Ocean is crucial to the I-to-A transition. When both interactive Indian and Pacific Oceans are included in the CGCM, the Indo-Pacific Run produces comparable numbers of A-to-I and I-to-A transition cases, similar

TABLE 1. Numbers of I-to-A and A-to-I transition cases identified in the observation (CMAP) and the CGCM runs.

	CMAP	Indo-Pacific run	Pacific run	Indian Ocean run
Length of time series (yr)	23	30	30	30
I-to-A transition case	6	11	7	3
A-to-I transition case	7	7	2	8

to the observations. Among the CGCM runs, only the Indo-Pacific run produces a biennial spectral peak (about 2.6 yr) in the IMRI and AMRI anomalies (not shown). The power spectra (not shown) of the monsoon indices show a 4-yr peak in the Pacific Run and are basically red in the Indian Ocean run.

Time-lag correlation coefficients between monthly IMRI and AMRI anomalies are calculated for the three CGCM runs and the CMAP observations. In the observations, Fig. 3a shows that there are two large correlation coefficients with the positive one occurring when the IMRI leads the AMRI by 5 months, and the negative one occurring when the IMRI lags the AMRI by 8 months. The positive time-lag correlation represents a tendency for a strong (weak) Indian summer monsoon to be followed by a strong (weak) Australian summer monsoon, that is, the in-phase I-to-A transition. The negative correlation represents the out-of-phase A-to-I transition. The Indo-Pacific run also produces one large positive and one large negative correlation coefficient at time lags close to those of the observations (Fig. 3b). Figure 3c shows that there is only one large correlation in the Pacific Run, which is positive and occurs when the IMRI leads the AMRI by 6 months. This in-phase I-to-A transition tendency does not occur in the Indian Ocean run (Fig. 3d). In this run, the largest correlation is negative and occurs when the AMRI anomaly leads the IMRI anomaly by 5 months. This negative correlation represents an out-of-phase transition from the Australian summer monsoon to the Indian summer monsoon.

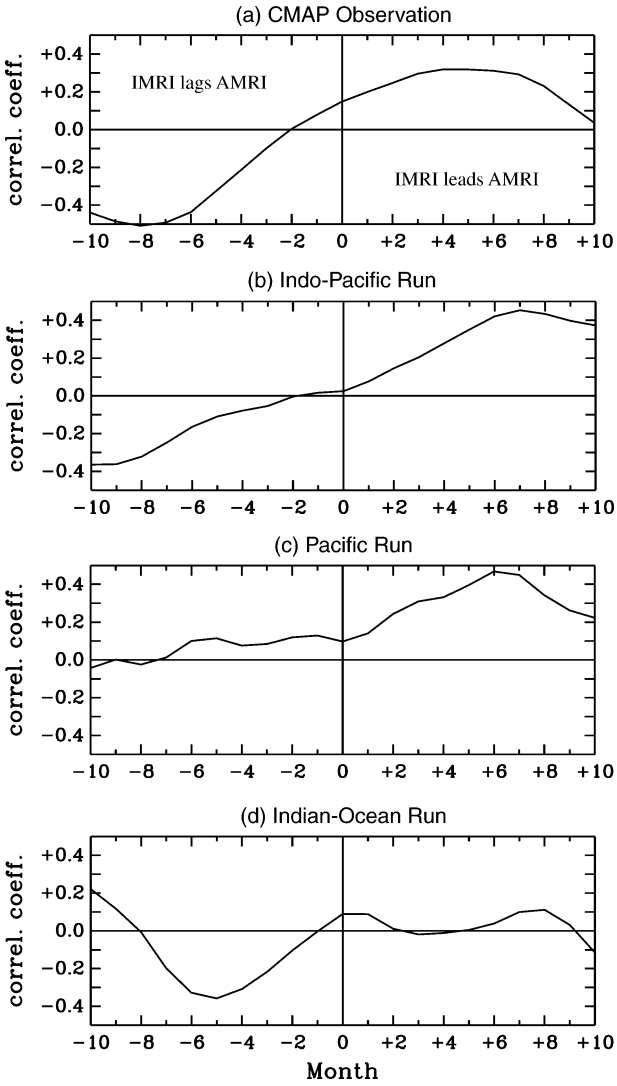

FIG. 3. Time-lagged correlation coefficients between monthly IMRI and AMRI calculated from the (a) CMAP observation, (b) Indo-Pacific run, (c) Pacific run, and (d) Indian Ocean run.

4. Associated SST anomalies in the Indian and Pacific Oceans

Composite maps are constructed to examine the associated SST anomalies in the Indian and Pacific Oceans during the A-to-I and I-to-A transitions. The transition cases identified in Fig. 2 are used to construct the composites. For the I-to-A transition, interannual SST anomalies are composited for the northern summer season (JJA), the northern autumn (SON), and the following southern summer (DJF). Composites are constructed separately for the ''positive'' (from a strong Indian monsoon to a strong Australian monsoon) and ''negative'' (from a weak Indian monsoon to a weak Australian monsoon) transition cases. Differences between these two composites (positive minus negative) are then calculated to identify the associated SST anomalies during the I-to-A transition. A similar procedure is followed for the A-to-I transition for the northern winter (DJF), the northern spring (MAM), and the northern summer (JJA) of the following year. The differences between the SST composite for the transition from a strong Australian monsoon to a weak Indian monsoon and that for the transition from a weak Australian monsoon to a strong Indian monsoon are calculated.

We first focus on the evolutions of composite SST anomalies during the I-to-A transition in observations and the two CGCM experiments that produce this type of monsoon transition: the Indo-Pacific run and the Pacific run. For the observations, SSTs from the Global Sea Ice and Sea Surface Temperature Data Set (GISST; Rayner et al. 1996) are composited for the I-to-A transition cases identified in Fig. 2a. Figure 4 shows that

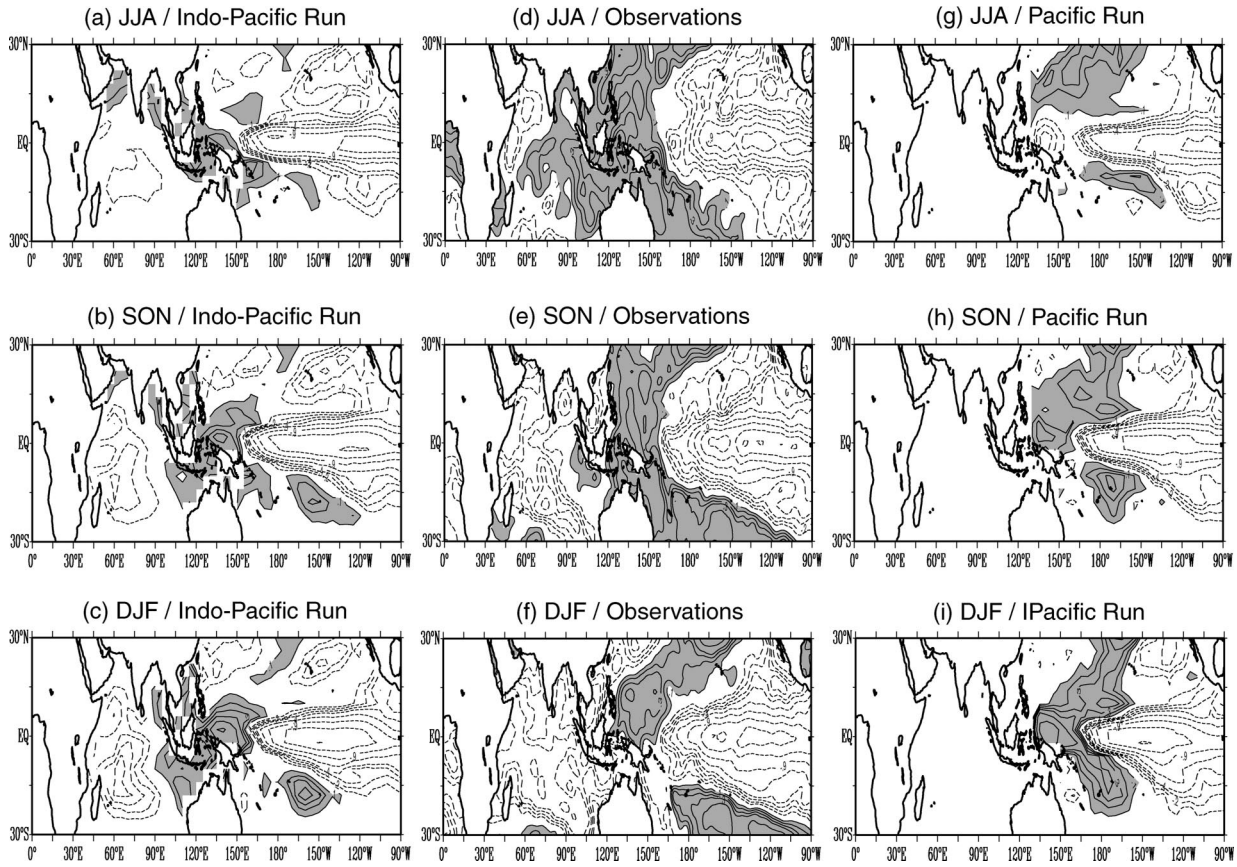

FIG. 4. Evolutions of interannual SST anomalies during the I-to-A transition. (a)–(c) Composited from the Indo-Pacific run, (d)–(f) from observations, and (g)–(i) from the Pacific run. SST anomalies are averaged for the seasons of JJA, SON, and DJF. Contour intervals are 0.1°C. Zero line is omitted. Positive values are shaded.

the major features of SST anomalies composited from the Indo-Pacific run (Figs. 4a–c) are, in general, close to those composited from the observations (Figs. 4d–f). These features include the following: 1) SST anomalies reverse sign in the Indian Ocean and 2) large cold SST anomalies persist in the Pacific Ocean from northern summer to southern summer. In the Indian Ocean, basinwide SST anomalies change sign from positive in the previous spring season (not shown) to negative in the strong Indian monsoon season (JJA). This sign reversal in the Indian Ocean SST anomalies is similar to that found by Meehl and Arblaster (2002a). They showed that the atmospheric circulation associated with the anomalous Indian summer monsoon initiates the SST transition in the Indian Ocean. Figure 4 shows that, during this sign-reversal period, SST anomalies in the Indian Ocean are relatively small and therefore presumably have a relatively weak influence on the atmosphere during the I-to-A transition. In the Pacific Ocean, the spatial pattern of the large SST anomalies resembles a La Niña event, with cold SST anomalies in the central-to-eastern sector and warm SST anomalies in the western sector. These SST anomalies are likely maintained by air–sea coupling in the Pacific from northern to southern summer. When the southern summer arrives, the SST anomalies in the Pacific Ocean increase the supply of water vapor to the Australian monsoon region and enhance the Walker circulation over the Pacific. Both effects result in a strong southern summer monsoon. In summary, the Pacific Ocean is more crucial than the Indian Ocean to the development of the in-phase transition from the Indian summer monsoon to the Australian summer monsoon. This explains why the Pacific run, but not the Indian Ocean run, produces the in-phase I-to-A monsoon transition frequently. The composite Pacific Ocean SST anomalies from the Pacific run during the I-to-A transition (Figs. 4g–i) are close to those of the Indo-Pacific run during this transition period.

For the A-to-I transition, we focus on the observations and the two CGCM experiments that produce this type of transition: the Indo-Pacific run and the Indian Ocean run. Figures 5a–c show that the major features of the composite SST anomalies from the Indo-Pacific run are characterized by a sign reversal of the anomalies in the Pacific Ocean, and large and persistent anomalies in the Indian Ocean. These SST anomaly features are close to those composited from the observations for the A-to-I

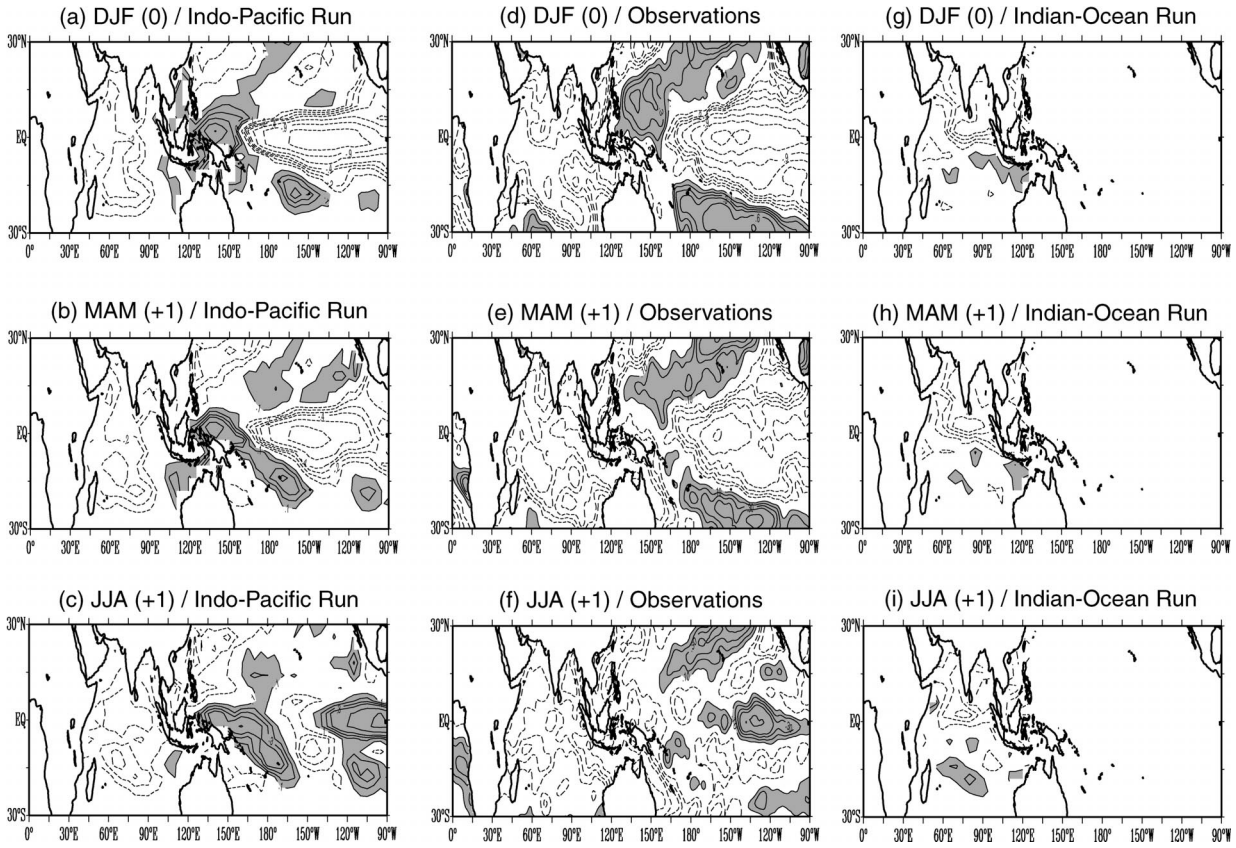

FIG. 5. Evolutions of interannual SST anomalies during the A-to-I transition: (a)–(c) composited from the Indo-Pacific run, (d)–(f) from observations, and (g)–(i) from the Indian Ocean run. SST anomalies are averaged for the seasons of DJF, MAM, and JJA of the next year (+1). Contour intervals are 0.1°C. Zero line is omitted. Positive values are shaded.

transition (Figs. 5d–f), although there are differences in detail. The cold SST anomalies in the Pacific weaken after the strong Australian monsoon season (DJF) and change to warm SST anomalies as the weak Indian monsoon season occurs (JJA). This is consistent with the finding by Meehl and Arblaster (2002a) that the Australian summer monsoon initiates the phase transition of Pacific SST anomalies. During this sign-reversal period, SST anomalies in the Pacific Ocean are relatively small and should have a relatively weak influence on the atmosphere. It is the Indian Ocean, which maintains large and persistent basinwide cold SST anomalies via coupled air–sea interactions, that is more crucial to the phase transition from the Australian summer monsoon to the Indian summer monsoon. When the northern summer arrives, these cold anomalies reduce the supply of water vapor to the Indian monsoon region and lead to a weak Indian monsoon in the JJA of the next year. Therefore, the Indian Ocean is more crucial than the Pacific Ocean to the development of the out-of-phase transition from the Australian summer monsoon to the Indian summer monsoon.

The Indian Ocean run also shows persistent and large cold SST anomalies in the Indian Ocean during the A-to-I transition (Figs. 5g–i). It is noted that the largest SST anomalies in this run are centered in the northern Indian Ocean. In the Indo-Pacific run, the largest SST anomalies are located in the tropical western Indian Ocean. This difference is likely due to the fact that ENSO influences are included in the Indo-Pacific run but excluded in the Indian Ocean run. We have shown in Yu et al. (2002) using this same CGCM that La Niña (El Niño) events tend to cool down (warm up) the tropical western Indian Ocean with a few months of time lag. The western Indian Ocean SST anomalies produced by the Indo-Pacific run during the A-to-I transition may be related to the La Niña–like SST anomalies in the Pacific during the same transition.

5. Conclusions and discussion

This study uses three CGCM experiments (i.e., Indo-Pacific, Pacific, and Indian Ocean runs) to examine the roles of the Indian and Pacific Oceans in affecting the transitions of the TBO in the Indian and Australian monsoon systems. Our results indicate that the Pacific Ocean and its air–sea coupling are more crucial than the Indian Ocean to the in-phase transition from strong (weak) Indian summer monsoons to strong (weak) Australian summer monsoons. On the other hand, the Indian Ocean

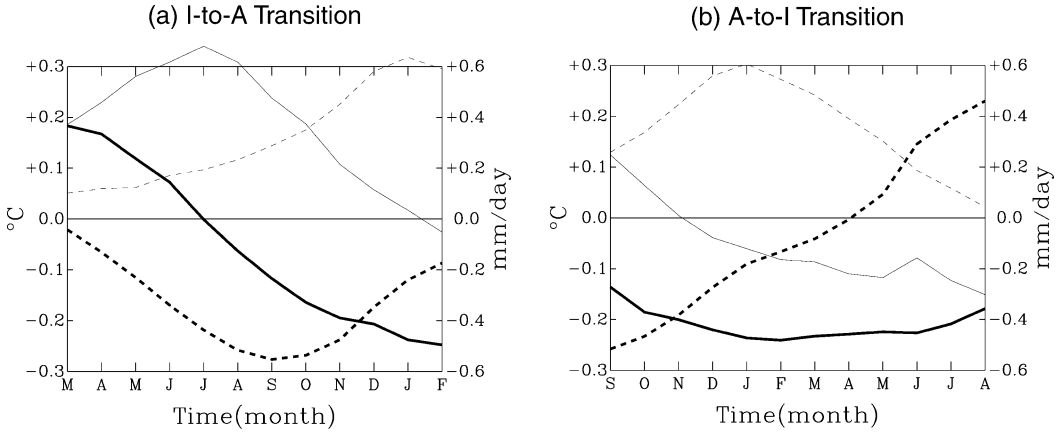

FIG. 6. Temporal evolutions of interannual anomalies in IMRI (thin-solid line), AMRI (thin-dashed line), central Pacific SST (thick-dashed line), and central Indian Ocean SST (thick-solid line) during the (a) I-to-A transition and (b) A-to-I transition. All values are composited from the Indo-Pacific run.

and its air–sea coupling are more crucial to the out-of-phase transition from strong (weak) Australian summer monsoons to weak (strong) Indian summer monsoons. When SST variations in both oceans are included, the Indo-Pacific run produces biennial variations in the Indian and Australian monsoons. A strong (weak) monsoon year is frequently followed by a weak (strong) monsoon year.

The different evolutions of the Indian and Pacific Ocean SST anomalies are the key that reveals the different roles of these two oceans in the transition phases of the TBO. Figure 6 is constructed to summarize these different SST evolutions and their relationships with the monsoon transitions. In this figure, the composited SST anomalies of Figs. 4 and 5 are averaged in the central Indian Ocean (20°S–20°N, 40°–80°E) and in the central Pacific Ocean (10°S–10°N, 150°E–170°W) for the I-to-A and A-to-I transitions in the Indo-Pacific run. The corresponding IMRI and AMRI values composited during those seasons are also shown in the figure. Figure 6a shows that after a strong (weak) Indian summer monsoon occurs, SST anomalies change sign in the Indian Ocean. SST anomalies are small during the in-phase transition in the northern autumn. During the same period, SST anomalies in the Pacific Ocean are large and contribute to the I-to-A transition. Figure 6b shows that, after changing sign in the Indian summer monsoon season, Indian Ocean SST anomalies continue to grow and reach large amplitude during the A-to-I transition. During this transition period, the Pacific SST anomalies change sign. SST anomalies in the Pacific are, therefore, small. The large Indian Ocean SST anomalies contribute to the out-of-phase transition from a strong (weak) Australian summer monsoon to a weak (strong) Indian summer monsoon.

Our results are consistent with the finding of Meehl and Arblaster (2002a) that the Indian and Australian monsoons play different roles in forcing the SST transitions in the Pacific and Indian Oceans during the TBO. Our results go further to show that SST feedbacks in these two oceans play different roles in the in-phase and out-of-phase transitions of the TBO in the Indian and Australian summer monsoons. Therefore, the TBO transitions in the Indian–Australian monsoon system are related to the seasonally dependent forcing and feedback between the monsoon systems and the Indo-Pacific Oceans. The Indian and Pacific Oceans have different potential to predict the interannual variations of Indian and Australian summer monsoons.

Acknowledgments. The authors thank anonymous reviewers for their suggestions on the improvements of this paper. The research was supported by the NOAA CLIVAR-Pacific Program under Grant NA16GP1016. Model integrations and analyses were performed at the San Diego Supercomputer Center and at the University of Michigan with computer allocations provided by the National Partnership for Advanced Computational Infrastructure (NPACI).

REFERENCES

Bryan, K., 1969: A numerical method for the study of the circulation of the world ocean. *J. Comput. Phys.*, **4,** 347–376.

Chang, C.-P., and T. Li, 2000: A theory for the tropical tropospheric biennial oscillation. *J. Atmos. Sci.*, **57,** 2209–2224.

Clarke, A. J., X. Liu, and S. V. Gorder, 1998: Dynamics of the biennial oscillation in the equatorial Indian and far western Pacific Oceans. *J. Climate*, **11,** 987–1001.

Cox, M. D., 1984: A primitive equation three-dimensional model of the ocean. GFDL Ocean Group Tech. Rep. 1, 141 pp.

Kalnay, E., and Coauthors, 1996: The NCEP/NCAR 40-Year Reanalysis Project. *Bull. Amer. Meteor. Soc.*, **77,** 437–472.

Kim, K.-M., and K.-M. Lau, 2001: Dynamics of monsoon-induced biennial variability in ENSO. *Geophys. Res. Lett.*, **28,** 315–318.

Mechoso, C. R., J.-Y. Yu, and A. Arakawa, 2000: A coupled GCM pilgrimage: From climate catastrophe to ENSO simulations. *General Circulation Model Development: Past, Present, and Future*, D. A. Randall, Ed., Academic Press, 539–575.

Meehl, G. A., 1987: The annual cycle and interannual variability in

the tropical Indian and Pacific Ocean regions. *Mon. Wea. Rev.*, **115,** 27–50.

——, 1993: A coupled air-sea biennial mechanism in the tropical Indian and Pacific regions: Role of oceans. *J. Climate*, **6,** 31–41.

——, and J. M. Arblaster, 2002a: The tropospheric biennial oscillation and Asian–Australian monsoon rainfall. *J. Climate*, **15,** 722–744.

——, and ——, 2002b: Indian monsoon GCM sensitivity experiments testing tropospheric biennial oscillation transition conditions. *J. Climate*, **15,** 923–944.

Mooley, D. A., and B. Parthasarathy, 1984: Fluctuations in all-India summer monsoon rainfall during 1871–1978. *Climate Change*, **6,** 287–301.

Nicholls, N., 1978: Air–sea interaction and the quasi-biennial oscillation. *Mon. Wea. Rev.*, **106,** 1505–1508.

Rayner, N. A., E. B. Horton, D. E. Parker, C. K. Folland, and R. B. Hackett, 1996: Version 2.2 of the Global Sea-Ice and Sea Surface Temperature Data Set, 1903–1994. Climate Research Tech. Note 74, Met Office, Bracknell, Berkshire, United Kingdom.

Ropelewski, C. F., and M. S. Halpert, 1987: Global and region scale precipitation patterns associated with the El Niño/Southern Oscillation. *Mon. Wea. Rev.*, **115,** 1606–1626.

Tomita, T., and T. Yasunari, 1996: Role of the northeast winter monsoon on the biennial oscillation of the ENSO/monsoon system. *J. Meteor. Soc. Japan*, **74,** 399–413.

Webster, P. J., V. O. Magana, T. N. Palmer, J. Shukla, R. A. Tomas, M. Yanai, and T. Yasunari, 1998: Monsoons: Processes, predictability, and the prospects for prediction. *J. Geophys. Res.*, **103,** 14 451–14 510.

Xie, P., and P. A. Arkin, 1997: Global precipitation: A 17-year monthly analysis based on gauge observations, satellite estimates, and numerical model outputs. *Bull. Amer. Meteor. Soc.*, **78,** 2539–2558.

Yasunari, T., 1990: Impact of Indian monsoon on the coupled atmosphere ocean system in the tropical Pacific. *Meteor. Atmos. Phys.*, **44,** 29–41.

——, and R. Suppiah, 1988: Some problems on the interannual variability of Indonesian monsoon rainfall. *Tropical Rainfall Measurements*, J. S. Theon and N. Fugono, Eds., Deepak, 113–122.

Yu, J.-Y., and C. R. Mechoso, 2001: A coupled atmosphere–ocean GCM study of the ENSO cycle. *J. Climate*, **14,** 2329–2350.

——, W. T. Liu, and C. R. Mechoso, 2000: An SST anomaly dipole in the northern subtropical Pacific and its relationship with ENSO. *Geophys. Res. Lett.*, **27,** 1931–1934.

——, C. R. Mechoso, J. C. McWilliams, and A. Arakawa, 2002: Impacts of the Indian Ocean on the ENSO Cycle. *Geophys. Res. Lett.*, **29,** 1204, doi:10.1029/2001GL014098.